

Vibration analysis of micro mirrors for LIDAR using on-chip piezo-resistive sensor

Jan Grahmann^a, Richard Schroedter^b, Oliver Kiethe^c, and Ulrich Todt^a

^aFraunhofer Institut for Photonic Microsystems (IPMS), Maria-Reiche-Str. 2, 01109 Dresden, Germany

^bTechnical University Vienna / Automation and Control Institute (ACIN), Gußhausstraße 27-29 / E376V, A-1040 Wien, Austria

^cFDTech GmbH, Bornauer Str. 205, 09114 Chemnitz, Germany

ABSTRACT

Novel research focuses on the use of micro scanning mirrors in mobile applications like automotive LiDAR sensors, head-mounted displays or portable micro beamer. Even under normal conditions, micro scanners are exposed to considerable environmental influences. Particularly disturbances such as shock, vibration and temperature fluctuations are relevant for miniaturized scanning systems. In this publication we show the critical environmental parameters for quasi-static micro mirrors with a staggered vertical comb drive intended for high-precision trajectory tracking control. Scanners are controlled based on a piezo-resistive position sensor feedback. Focus will be experimental shock and vibration analysis by exposure to sinusoidal and wide-band random vibration excitation as typical for automotive industry specifications. These are the most demanding requirements compared with other application fields of MEMS mirrors. The on-chip piezo-resistive sensor enables evaluation of the vibration load on the micro scanner, without any optical measurement setup. MEMS mirrors are mounted on a shaker system for characterization and are attached to a vehicle body to evaluate a real application scenario. Furthermore the performance in open-loop and closed-loop control mode is analyzed and shows very good applicability of micro scanners in an automotive environment.

Keywords: MEMS-Scanner, LIDAR, vibration, electrostatic, reliability, trajectory precision, quasi-static

1. INTRODUCTION

MEMS scanning mirrors have been around for over two decades. Different applications have driven the development of this technology, bringing into the field not only development organizations like universities and institutes, but also companies trying to make a business. Driver for the technology in the early 2000s was for example barcode scanning,¹ a 1D application with a scanning frequency of a couple hundred hertz. Much more sophisticated scanner designs were necessary to serve the next driver, mobile laser projection.²⁻⁴ The business scenario was, to have a mobile laser projector in each smart phone sold like the cameras today. Due to the necessity of frequency doubling lasers for green light at the time and issues of a too large power consumption, cost and missing miniaturization to truly integrate the mobile projection engine completely into a 7 mm thin smart phone, the business case had not evolved as expected. Also the resolution of displays had considerably increased in the meantime and therefore raised the technical requirements to achieve true HD. Besides this large consumer application there are many applications with a smaller market like microscopy, tunable laser sources,^{5,6} spectroscopy⁷ or different applications in the medical field like e.g. endoscopy or OCT. Typical for these applications are much smaller numbers of MEMS-scanners needed per year, but with a strong need of customization to fulfill their specific technical requirements. Two drivers have become more dynamic within the last 3 years approximately. One are head mounted displays, requiring small and fast scanning mirrors (mirror diameter typically < 2 mm) and a second is LIDAR (Light Detection and Ranging) with typically larger required mirror plates from 3 mm to 20 mm, depending on the system concept, addressed detection range and used detection method. LIDAR

Send correspondence to Dr. Jan Grahmann

E-mail: jan.grahmann@ipms.fraunhofer.de, Telephone: 0049 351 8823 349

as driver assistance or for future autonomous driving, measures the distance to surrounding objects, creating a 3d-map. The LIDAR-engine has to be integrated into the automotive environment, which is why reliability issues become very important, ranging from temperature, humidity to mechanical shock and vibration. The automotive industry is a very demanding market in this respect. That is why the LIDAR community discusses the question of a Solid State LIDAR (A LIDAR without moving parts), despite of the fact that most LIDAR systems nowadays are based on a scanning lidar either using conventional technologies like galvanometer and polygon scanners or MEMS-scanners. The scanning represents a spatial filter for either the emitted light (transmitting channel) or also for the detected light (receiving channel) and therefore enhances the signal to noise ratio for the LIDAR-detector. That is why the question is not, whether the used LIDAR approach is solid state or not, but does it withstand reliably the shock and vibration requirements of the automotive industry? The following sections provide a contribution to answer this question, in this case for electrostatic driven bulk single crystal silicon MEMS scanners, developed at IPMS.

2. SHOCK AND VIBRATION REQUIREMENTS FOR AUTOMOTIVE AND TEST CONDITIONS

Different standards (DIN EN 60721-3-1-5,⁸ LV124;⁹ JESD22-B103B;¹⁰ MIL-STD-883;¹¹ AEC Q100¹²) have been evaluated according to their applicability for shock and vibration analysis of MEMS-scanners. Whereas LV124 is a specification of leading German automotive manufacturers with the requirements and test descriptions for components used in cars up to 3.5 t. This was mainly used as reference for the following test scenarios. Thereby it needs to be noticed that **these requirements are for destructive reliability tests**. The standards categorize the load requirement, where in the following only the categories with the highest load are given. Meaning the DUT (Device Under Test) does not necessarily have to survive the explicit test load in order to pass a test. It is therefore sufficient to document the test load that was survived by a DUT. This is true for shock testing. Performing vibration testing has two aspects. One is for the DUT to survive the test load undamaged. The second is to determine how the trajectory precision is affected by the vibration loads. In order to fulfill typical LIDAR requirements the angular trajectory precision should achieve a resolution of $\leq 0.1^\circ$.

2.1 Mechanical shock

Shock test requirements, for example simulating the mechanical load on components when driving over curbs or in accidents, are shown below according to LV124.

Table 1: Test parameters mechanical shock LV124

peak acceleration	$500 \frac{\text{m}}{\text{s}^2}$ (50 g)
shock duration	6 ms
shock form	Half-sine
number of shocks	10
number of DUTs	6

Comparing the requirement of table 1 with the shocktest in figure 1, that is conducted according to MIL-STD-883E, it can be seen that the automotive requirements of 50 g and 6 ms pulse width are far exceeded by the tested slow frequency (100 Hz) soft spring scanning mirror. The shown 2500 g at a pulse width of 0.7 ms are an internal IPMS standard, that should be achieved for a robust scanner design. Figure 1b shows that first failures for this soft scanner design occur at 3500 g. Whereas the color presents the load direction for the scanner. The most critical one is typically the z-direction being the normal of the mirror plate. This is also represented by the shock test results. Since MEMS-scanners with eigenfrequencies below 100 Hz are typically not designed at IPMS, above all because lower scan frequencies can be addressed by quasi-static mirrors holding the eigenfrequency above 100 Hz, this is basically a robust device type. In a LIDAR application larger mirror diameters are advantageous at large field of views e.g:

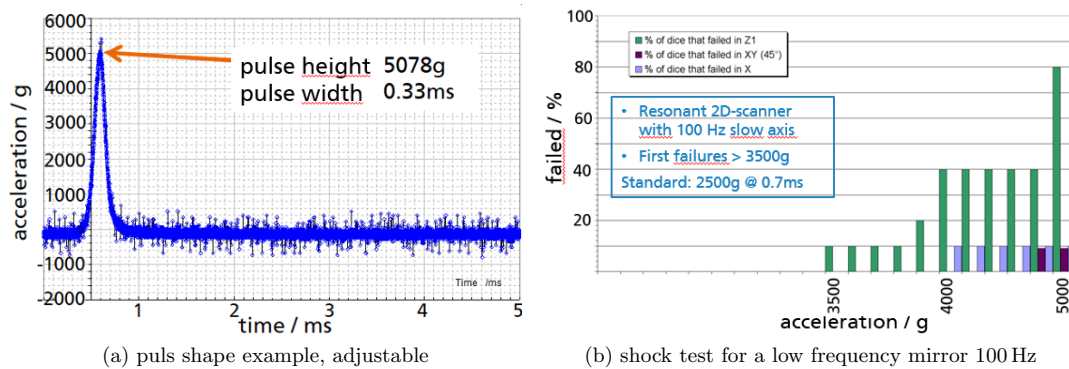
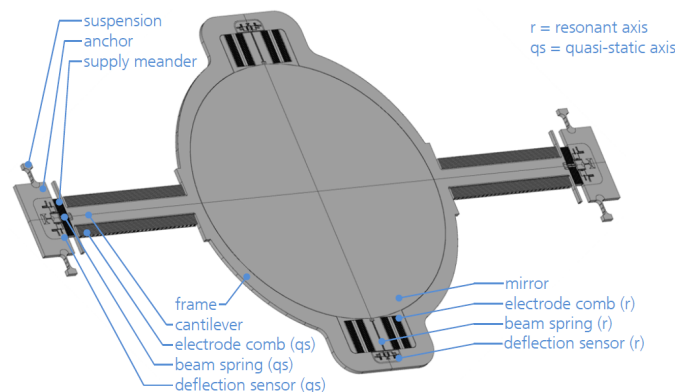


Figure 1: Shock test according to MIL-STD-883E on Spectra ENDEVCO POP 2925 equipment

13

- horizontal field of view: $60^\circ - 360^\circ$,
- vertical field of view: $20^\circ - 40^\circ$,
- typical mirror diameters 3 mm – 6 mm,
- larger mirror diameters from 10 mm – 20 mm are also very desired,

but according to cost and miniaturization advantage the latter is not sensible as monolithic MEMS-scanner. There are hybrid approaches to offer larger mirror diameters and at the same time use the excellent mechanical characteristics of single crystal silicon for the mirror plate and springs. A separated driving mechanism that is attached to the silicon by assembly processes. However, automated precise and low cost assembly for large quantities is necessary, while also ensuring reliable assembly interfaces. This is key for a potential success of this approach. Another drawback of large mirror diameters is, that chip size goes directly proportional into cost for the semiconductor respectively MEMS-business, potentially compensating the cost scaling advantage of semiconductor technologies. A quasi-static resonant MEMS-scanner placed with a mirror plate diameter trade off for a monolithic approach within the LIDAR requirements is shown in figure 2.

Figure 2: Monolithic large MEMS mirror design with 5 mm mirror plate, FOV of $90^\circ \times 40^\circ$ and a quasi-static scan, up to 35 Hz plus resonant horizontal scanning at 363 Hz withstanding shock of 2500 g, according to simulation.

2.2 Vibration loads

The sinusoidal vibration loads for the different standards mentioned, range in between 20 g – 70 g depending on the frequency range to be swept for testing to find the critical frequencies for the device under test (DUT). Besides an acceleration level to be used for the vibration test also displacements to excite the DUT are described, that range again depending on the frequency range, at low frequencies between 7.5 mm for 2 Hz – 8 Hz down to 0.75 mm at frequencies beyond 20 Hz. The noise vibration load according to LV124 is shown in figure 3.

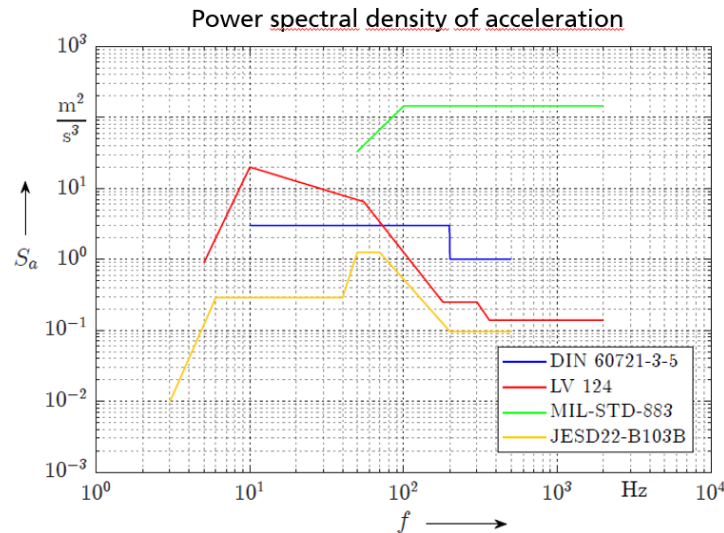


Figure 3: Power spectral density acceleration requirements for different standards

2.3 Test conditions

For the here described vibration analysis the critical frequencies were well known due to the FEA-modal analysis. The eigenfrequencies were verified by frequency sweeps on a shaker. At the parasitic mode frequency the scanners were tested at different acceleration levels up to 30 g non-operating and operating to determine the influence on the scan trajectory (see section 4). **This is a real worst case test, since these acceleration levels are actually mandatory to determine and compare the vibration resistance of different device manufacturers regarding fatigue or other reliability issues that lead to a damaged component and not to measure, how much the operation of the DUT will be influenced without damaging it.**

The same is true for wideband noise vibration loads. These give a more realistic scenario of load spectra that could occur during operation, but the intensity of the test loads is much higher in order to accelerate issues like fatigue. The different standards are shown in figure 3. The standard LV124 is used for the wideband noise vibration testing described in section 5 and is intended for hang-on parts (for components installed on sprung masses).

The testing was done on an electrodynamic shaker system. The driving electronics and driver software for the MEMS-scanners were modified to track and store the differently oriented movements of the scanner into parasitic directions, besides the rotational θ -deflection. The integrated piezo-resistive position sensor was used to detect the deflection amplitudes for the different scanner movements. That is a precondition for testing, since an optical position feedback would very strongly increase the necessary effort for the test set up. The sensor resolution allowed to detect movements in the single mdg- and sub micrometer range.

3. DEGREES OF FREEDOM AND PARASITIC MODE CONSIDERATION

Vibration load spectra for a scanner design should be considered already during the design phase of the scanning micro mirror. In order to do this, it is necessary to simulate the eigenmodes of a mechanical component in this case a MEMS scanning mirror. This is a standard and it is available in all typical FEA-simulation programs. For resonant oscillating scanning mirrors this eigenmode analysis and comparing the results with the expected vibration spectra is the main part. Thereby the eigenfrequencies of the design should be placed into a frequency range where they are not excited too much to influence the oscillation of the scanner. Helping in the resonant case is, that the torsional eigenmode used for resonant operation typically has a quite high quality factor (even for scanning in atmosphere) in the range of hundred to a few hundred. The scanner acts therefore as small bandwidth filter, damping parasitic excitations when operating and parasitic eigenfrequencies in the 1D-case are movable to higher frequencies in the design phase. More critical is the quasi-static axis of the scanner, because it is operated away from its eigenfrequencies and the damping is necessary and used to control the trajectory precision. Therefore the following results are focused on vibration analysis of quasi-static scanners and the analysis of resonant scanner axis and 2D-scanning observations follows in the future.

Figure 4a shows a schematic of a 1D quasi-static scanner with its different degrees of freedom and corresponding mode shapes of an example scanner design. These mode shapes are for each design at different eigenfrequencies. Where table 2 shows three scanner examples that were analyzed with their different eigenfrequencies corresponding to the shown mode shapes.

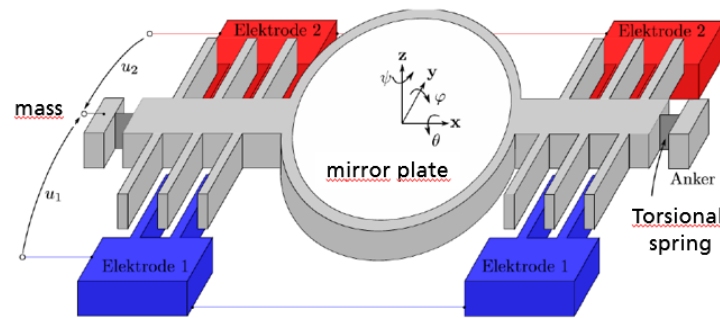
Table 2: Eigenfrequencies for three scanner designs with different torsional spring stiffness

Design	f_θ in Hz	f_ψ in Hz	f_x in Hz	f_y in Hz	f_z in Hz
Scanner 1	127	4083	14 605	1925	1319
Scanner 2	255	3519	19 364	2821	1187
Scanner 3	509	10 332	79 798	4868	3096

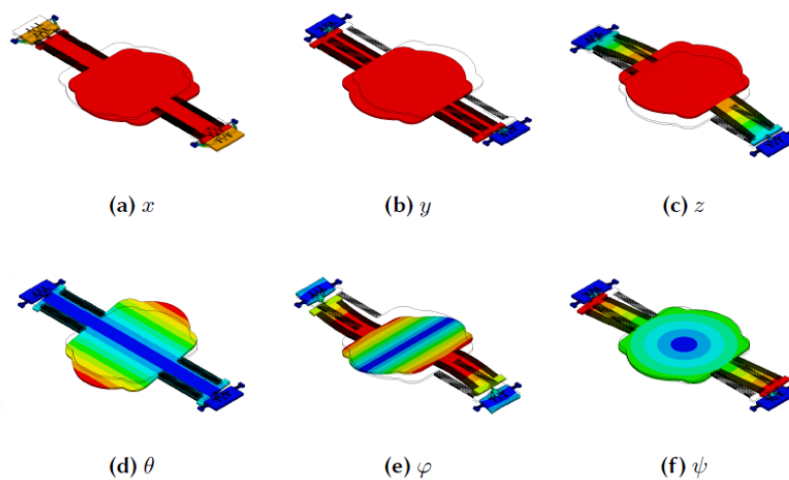
The torsional mode used for operation of the scanner is shown in figure 4b (d). Parasitic mode shapes according to their increasing frequency that could damage the scanner are in y- and z-direction as well as twisting in plane mode around z which is named ψ . These parasitic modes should not be excited over a certain threshold of amplitude, because all three have the potential to destroy the scanner or at least influence the trajectory precision. An oscillation in y lowers the small distance between the combs and in case they touch, it would come to a mechanical or an electrical damage. The same is true for the higher frequent ψ mode shape in figure 4b (f). This is a mode shape that, due to the decreasing distance between the side walls of the comb drive, encourages a pull-in of the scanner. The vertical movement of the mirror platen in z-direction also named pumping mode could cause damage in the anchoring of the mirror plate when the maximum stress limit of the single crystal silicon is exceeded by the mode amplitude. The inplane mode in direction of x in figure 4b (a) and the higher order bending mode φ shown in figure 4b (e) are much stiffer and have a higher frequency than the ones described before. So these latter two can be neglected for the further analysis and focus is on y-, ψ - and z-modes. Thereby it has to be seen that for an ideally symmetric mirror geometry with perfectly homogeneous mass distribution around the centre of gravity the translational vibration load could not excite a rotation and therefore a mirror deflection. However, for the non-perfect symmetric device an effect on the mirror deflection is possible in the case of a non-driven mirror. In case of an operated mirror, the equation of motion of the different degrees of freedom are coupled via the electrostatic drive. More sensitive to this coupling are soft spring, low frequency mirrors.

4. SINUSOIDAL VIBRATION TESTING

As described in section 2.3 the following sinusoidal exciting vibration loads were used in order to determine the influence on the trajectory precision and not in order to find the load that finally destroys the mirror mechanically.



(a) The six degrees of freedom of a quasi-static MEMS-scanner



(b) Eigenmode shapes

Figure 4: DOF and eigenmode shapes of a quasi-static MEMS-scanner

Nevertheless it can be stated, that the tested mirrors survived all vibration loads up to 30 g, independent on the different scanner designs and therefore mechanical spring stiffness. In order to completely comply to the test conditions of LV124 the test duration would have to be extended up to 8 hours. However compared to other DUTs for automotive it is special about the scanning micro mirrors that they are out of single crystal silicon which has got perfect characteristics regarding fatigue. The mirrors break when the maximum stress limit of the material is exceeded, but they do not show fatigue or creep due to the almost ideal proportionality of elasticity (Hooke's law). Hence, one would not expect a damaged mirror at a longer test duration than the here used one. Since it was already stated, that the mirrors were not damaged by the excitement of their parasitic modes in y- z- and ψ - degree of freedom at the following shown load levels, the interesting question was how much the rotational scan direction would be influenced by the translational excited modes. To compare the sensitivity of different stiff mirrors (varying eigenfrequency) without the influence of a driving signal, the sinusoidal vibration load was applied to non-operating mirrors (see figure 5). It can be seen that the excitation in y causes a slightly higher deflection angle of the MEMS-mirror than a vibration load in z-direction, each at the torsional resonance frequencies of the mirror. Secondly it is apparent that mirrors with lower torsional resonance frequency are much more sensitive and show higher deflection for example for y-vibration of up to 0.3° for the 127 Hz eigenfrequency mirror compared to 0.07° for the 503 Hz eigenfrequency mirror. For the next sinusoidal vibration test the scanners were driven with a linear triangle trajectory at 10 Hz and the linearity deviation at vibration loads in y- and

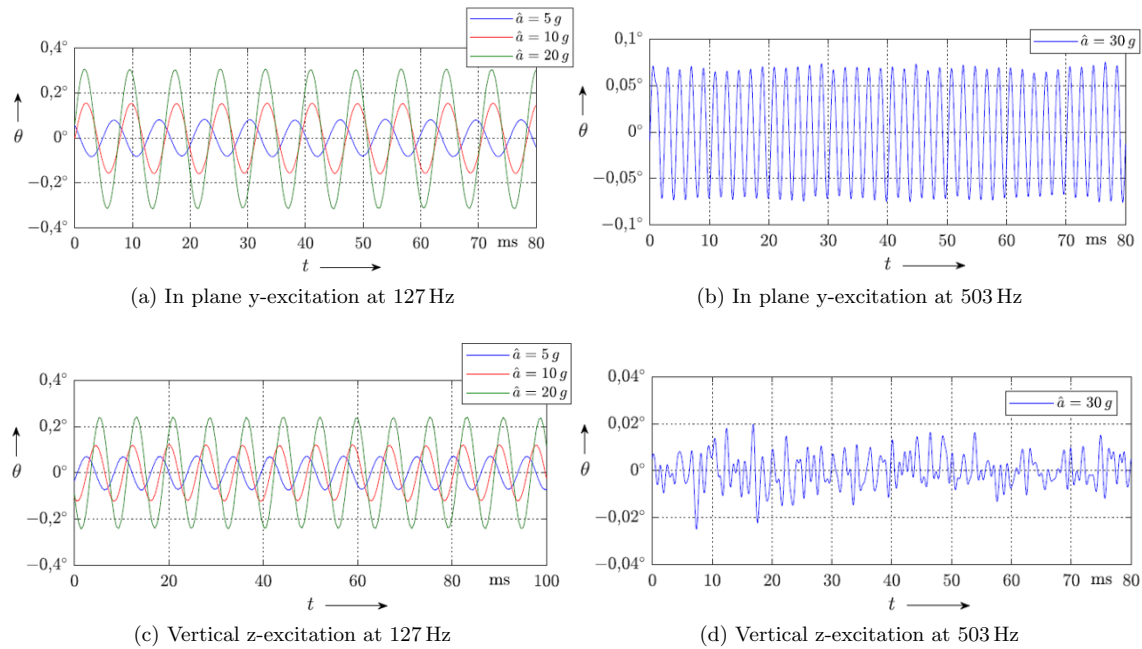


Figure 5: Mirror rotation deflection θ with in plane y and vertical z vibration excitement for **non-operating** scanner 1 and 3 with an exciting frequency at their rotational resonances f_θ

z-direction was measured for the open loop and closed loop case (figure 6 and figure 7).

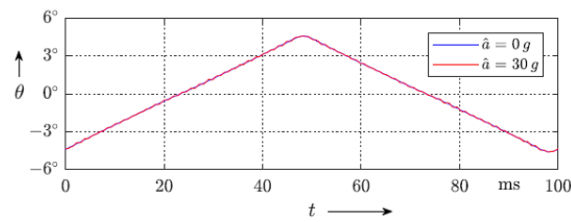
The measurement results show that:

- the deflection angle caused by vibration is clearly lower for operating than for non-operating mirrors at the same vibration loads,
- the closed loop operation reduces the linearity deviation by about 25% for z-vibration loads and about 50% for y-vibration loads.

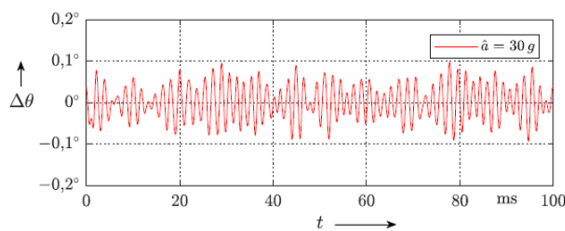
The reduction of linearity error between open and closed loop not only depends on the eigenfrequency of the scanner design, but also on the control sample frequency of the feedback loop and the feedback signal itself. Though the deflection in z- and y- for different vibration loads were measured, this signal was not used to improve controllability of the scanner. For the trajectory precision only the detected deflection for θ was used as feedback signal. To consider a feedback for parasitic movements and increase the control sample frequency has therefore the potential to improve the trajectory precision in closed loop further.

5. NOISE VIBRATION TESTING

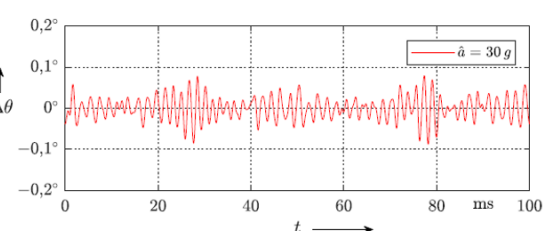
As described in section 3, the equation of motion for the different degrees of freedom are coupled via the capacitance of the electrostatic drive and can therefore lead to trajectory deviations, as also seen in the sinusoidal vibration test. In the following analysis the normal to the mirror plate surface (z-direction) was chosen to apply a noise vibration load according to LV124. This direction was chosen, because of the lower eigenfrequency from y- and ψ -modes and because of the larger movement in z compared with the other mode amplitudes. These determined by a greatly enhanced simulation model of the IPMS mirrors towards the consideration of vibration loads and their effect on scanning mirrors, using the here described vibration analysis results. So the z-direction was considered to be the most critical for the mirror. The LV124 vibration load shown in figure 8a was increased



(a) Triangular test trajectory with reference 0 g and 30 g vertical vibration load

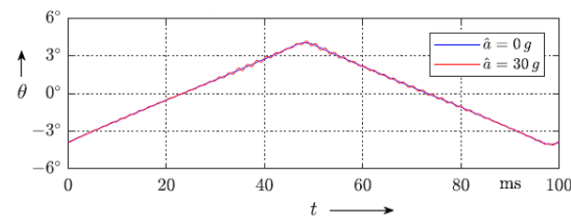


(b) Linearity error in open loop operation

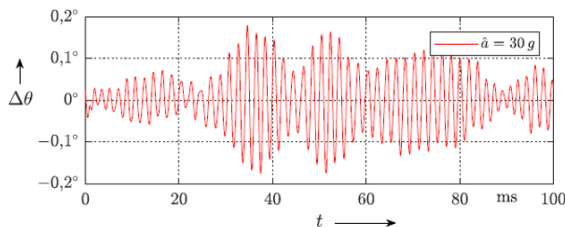


(c) Linearity error in closed loop operation

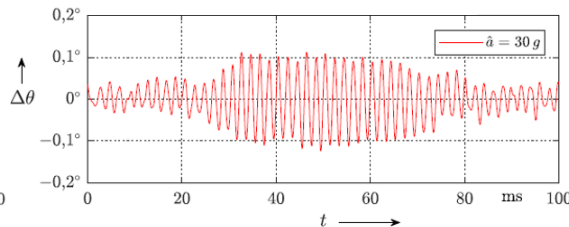
Figure 6: Vertical z-vibration load for mirror in operation



(a) Triangular test trajectory with reference 0 g and 30 g In-plane vibration load



(b) Linearity error in open loop operation



(c) Linearity error in closed loop operation

Figure 7: In-plane y-vibration load for mirror in operation

in three steps 25%, 50% and 100%. The sensor signal was used to determine the z-deflection and to measure the effect on the rotational deflection θ in the non-operating and operating case. A FFT of the signal for scanner 2 with its quite low rotational eigenfrequency of 255 Hz is plotted in figure 8b. The scanner is not operated, so that θ only represents the deflection excited by the vibration load. Important is to notice that the blue curve shows peaks, although it was measured without an exciting vibration load. This is due to the non-perfect lab environment, the shaker equipment was placed in, causing an EMC-issue. The red vertical line shows the rotational resonance frequency of the scanner and the two green frequency spectra show the rotational deflection

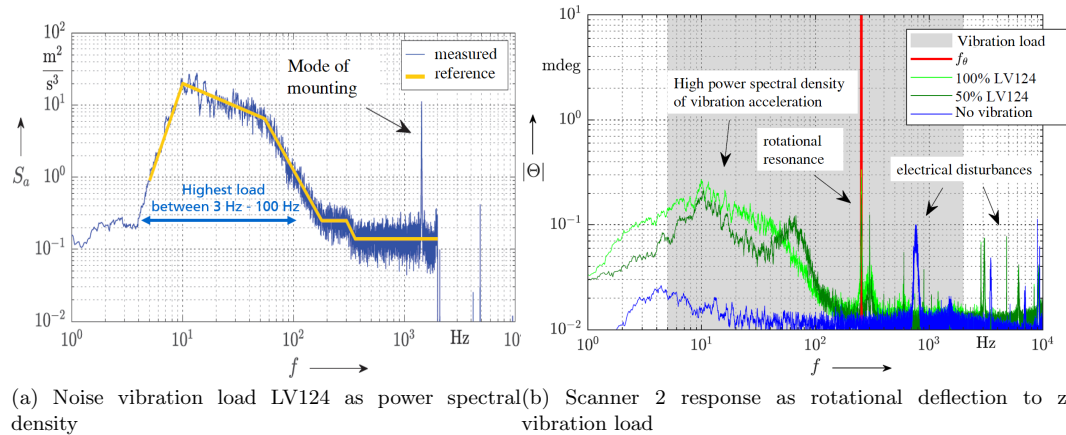


Figure 8: Noise vibration load requirements and MEMS-mirror response to z-vibration, scanner 2 without operation

in milli-degree. So it can be stated:

- vibration caused deflections are located in between 5 Hz – 100 Hz where the power spectral density is highest and at resonance frequency as long as it is in between the load frequency range,
- although a soft spring mirror is tested, the deflections are small,
- the scanner is not damaged by the actually for destruction intended vibration load.

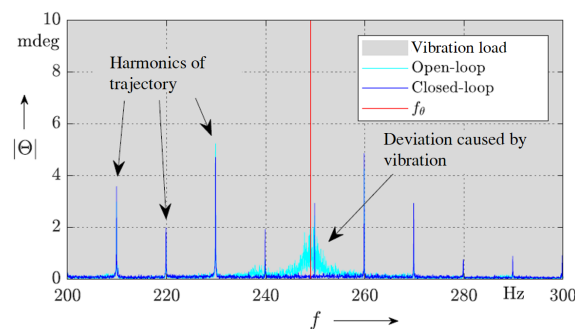


Figure 9: Amplitude spectrum of θ for scanner 2 in quasi-static operation (triangular scan), exposed to LV124 vertical noise vibration load (z-direction)

Measuring the mirror response in operation is shown in figure 9. Only the interesting frequency range with mentionable frequency shares are shown. The light blue shows the frequency shares for the open loop case and the dark blue for the closed loop case. The red line shows the resonance frequency. The light and dark blue curves are almost identical and show both the harmonics of the quasi-statically driven triangular trajectory. Around the resonance, the open loop curve shows a wider frequency band than in the closed loop case. These frequency shares contribute to the trajectory deviation, which in conclusion shows that the closed control loop with the narrow frequency peak at resonance strongly reduces the trajectory deviation caused by the vibration load.

6. ON ROAD OPERATION TESTING

In order to find out, what is a realistic vibration spectrum in a car and how the MEMS-scanner would respond to it, a scanner set up was attached to a car window. This was done to simulate the attachment of a scanning LIDAR to the car body. This set up was equipped with a three axis acceleration sensor to determine the vibration. The bumpiest road in Dresden was chosen to determine the vibration load and the results are shown for the acceleration level in the three axis in figure 10b. The vibration level is about two orders of magnitude

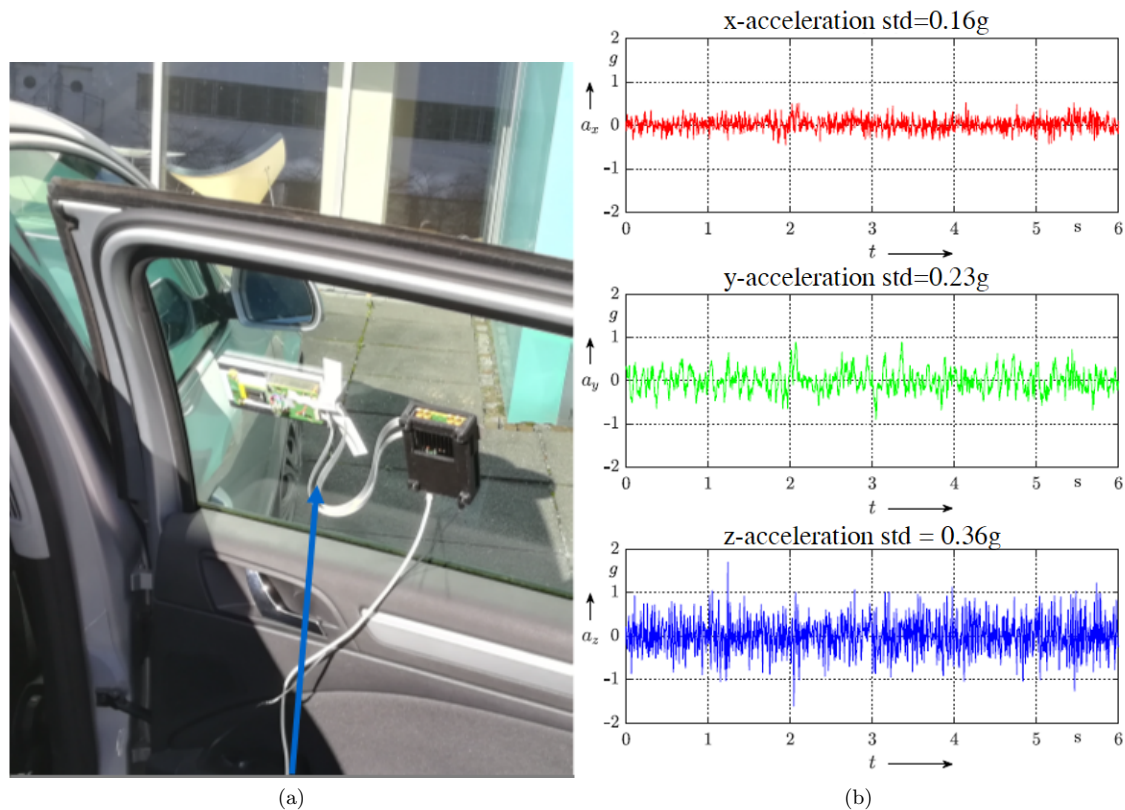


Figure 10: Measured acceleration level of a car window on bumpiest road in Dresden

lower than the vibration loads, that were used in sinusoidal and noise vibration testing described in section 4 to 5. This comparison is also shown by figure 11. These very low vibration loads are correlated well with the measured influence on the trajectory precision of the scanner operated during the drive. It was not possible, even for the lowest frequency scanner 1 to create a reduction of trajectory precision or measure any other deviation by the vibration loads the scanner was exposed to by driving the car.

7. CONCLUSION AND OUTLOOK

The described testing of electrostatic MEMS-mirrors allows the following conclusions:

- automotive shock requirements can be easily passed by the standard shock resistance of the scanners at 2500 g,
- the scanners were not damaged by the vibration loads, actually intended to compare maximum failure limits,

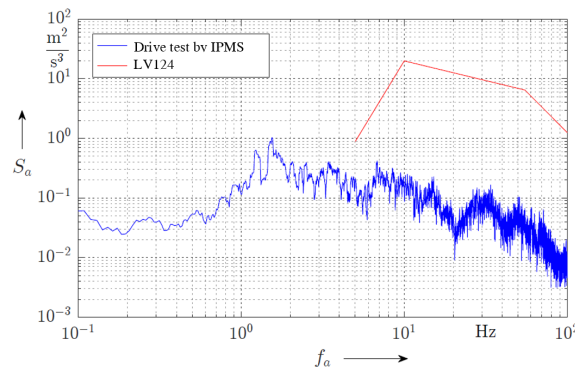


Figure 11: Measured vibration power spectral density of a car on bumpiest road in Dresden compared with LV124 requirements

- the vibration loads to which a scanner is realistically exposed during operation on a vehicle body, are about two orders of magnitude lower than the vibration loads of the standards,
- **there was no measurable influence on the scanner trajectories while driving the car,**
- with the vibration loads of LV124 the trajectory precision can deviate slightly, due to excitation of parasitic modes in z , y , and ψ direction,
- the softer the scanner (slower frequency), the higher the effect on the trajectory, here reported maximum is 0.3° for the 127 Hz scanner 1 at 20 g sinusoidal vibration load,
- the scanner models have been developed further to enable vibration simulation and its effect on the translational movement as well as the effect on the trajectory precision,
- no influence at all, even for the high vibration loads of LV124, is seen beyond an eigenfrequency of 2 kHz,
- the effect on the scanner trajectory even in open loop for the LV124 standard is still neglectable for the LIDAR application for eigenfrequencies beyond 500 Hz,
- the trajectory deviation with LV124 vibration loads can be strongly reduced in closed loop operation.

In the future 1D resonant scanners for comparison and 2D scanners will be tested and reported.

REFERENCES

- [1] Wolter, A., Schenk, H., Gaumont, E., and Lakner, H., "The mems micro scanning mirror for barcode reading: From development to production," in [*MOEMS Display and Imaging Systems II*], *Proceedings of SPIE* **5348**, 32–39 (2004).
- [2] Scholles, M., Bräuer, A., Frommhagen, K., Gerwig, C., Lakner, H., Schenk, H., and Schwarzenberg, M., "Ultracompact laser projection systems based on two-dimensional resonant microscanning mirrors," *Journal of Micro/Nanolithography, MEMS, and MOEMS* **7**(2), 021001–021001–11 (2008).
- [3] Kilcher, L. and Abelé, N., "Mems-based microprojection system with a 1.5cc optical engine," in [*MOEMS and Miniaturized Systems XI*], *Proceedings of SPIE* **8252**, 825204–1–825204–6, Society of Photo-Optical Instrumentation Engineers -SPIE, Bellingham, WA (2012).
- [4] Hung, A., Lai, H., Lin, T.-W., Fu, S.-G., and Lu, M., "An electrostatically driven 2d micro-scanning mirror with capacitive sensing for projection display," *Sensors and Actuators A: Physical* **222**, 122–129 (2015).
- [5] Grahmann, J., Merten, A., Herrmann, A., Ostendorf, R., Bleh, D., Drabe, C., and Kamenz, J., "Large moems diffraction grating results providing an ec-qcl wavelength scan of 20%," in [*MOEMS and Miniaturized Systems XIV, Proc. of SPIE*], *Proceedings of SPIE* **9375** (2015).

- [6] Ostendorf, R., Butschek, L., Hugger, S., Fuchs, F., Yang, Q., Jarvis, J., Schilling, C., Rattunde, M., Merten, A., Grahmann, J., Boskovic, D., Tybussek, T., Rieblinger, K., and Wagner, H.-J., "Recent advances and applications of external cavity-qcls towards hyperspectral imaging for standoff detection and real-time spectroscopic sensing of chemicals," *Photonics* **3**(2, 28) (2016).
- [7] Pügner, T., Knobbe, J., Grüger, H., and Schenk, H., "Design of a hybrid integrated mems scanning grating spectrometer," in [*Optical Design and Engineering IV, Proc. of SPIE*], *Proceedings of SPIE* **8167**, 816718–1–7 (2011).
- [8] Deutsches Institut für Normung, "Klassifizierung von umweltbedingungen. teil 3: Klassen von umwelteinflußgrößen und deren grenzwerte, hauptabschnitt 1: Langzeitlagerung," (1998-03).
- [9] Volkswagen AG, "Electric and electronic components in motor vehicles up to 3,5 t – general requirements, test conditions and tests," (2013-02-28).
- [10] JEDEC Solid State Technology Association, "Vibration, variable frequency," (2006-06).
- [11] MIL-STD-883, [*TEST METHOD STANDARD MICROCIRCUITS*], US Department of Defense (1996).
- [12] Automotive Electronics Council, "Failure mechanism based stress test qualification for integrated circuits," (2014-09-11).
- [13] Grahmann, J., Graßhoff, T., Conrad, H., Sandner, T., and Schenk, H., "Integrated piezoresistive position detection for electrostatic driven micro scanning mirrors," in [*MOEMS and Miniaturized Systems X, Proc. of SPIE*], *Proceedings of SPIE* **7930**, 79300V–1 – 79300V–8 (2011).